



ELSEVIER

Contents lists available at ScienceDirect

MethodsX

journal homepage: www.elsevier.com/locate/mex

Method Article

Selective laser assisted impairment of reverse osmosis membranes



Bogdan C. Donose^{a,*}, Ashwin Vijayan Premavally^{a,b}, Marie-Laure Pype^b,
Katrin Doederer^b

^aSchool of Chemical Engineering, The University of Queensland, St Lucia, QLD 4067, Australia

^bAdvanced Water Management Centre, The University of Queensland, St Lucia 4067, Australia

A B S T R A C T

Monitoring the loss of integrity in reverse osmosis (RO) membranes is crucial for protection of public health as small imperfections can result in catastrophic pathogen outbreaks. However, understanding the phenomena accompanying the loss of integrity in RO membranes relies on properly characterizing and interpreting performance data. Reproducing chemical and mechanical damage in model membranes that mimic the conditions of real-time operation is difficult. Mechanical impairment is particularly challenging, since one needs to damage selectively and in a controlled manner (producing holes of desired size) the barrier (polyamide) and/or the support layer (polyether sulfone and polyester). In this work we develop a straightforward approach to produce arrays of micro-holes in a commercially available RO membrane employing nanosecond pulsed laser ablation. The new approach is used to prepare four samples with different number of holes with constant diameter and increasing hole depth. These samples were further tested to reveal the impairment impact on filtration performance. It was observed that the flux was linked with the laser pulse density/penetration.

- Uniform radius defects were created in RO membranes.
- Higher pulse density leads to deeper defects.
- Ablation of all three layers can be attained.

© 2020 The Author(s). Published by Elsevier B.V.
This is an open access article under the CC BY-NC-ND license.
(<http://creativecommons.org/licenses/by-nc-nd/4.0/>)

A R T I C L E I N F O

Keywords: Integrity, Filtration, Water

Article history: Received 13 November 2019; Accepted 30 January 2020; Available online 21 February 2020

* Corresponding author.

E-mail addresses: bogdan.donose@unimelb.edu.au, b.donose@uq.edu.au (B.C. Donose).

Specification Table

Subject Area:	Chemical Engineering
More specific subject area:	<i>Desalination by reverse osmosis</i>
Method name:	<i>Laser impairment of reverse osmosis membranes</i>
Name and reference of original method:	<i>Pontius, F.W., J.P. Crimaldi, and G.L. Amy, Virus passage through compromised low-pressure membranes: A particle tracking model. Journal of Membrane Science, 2011. 379(1): p. 249–259</i>
Resource availability:	<i>A full description of the details is provided in the manuscript</i>

Method details

High-pressure membranes such as reverse osmosis (RO) and nanofiltration (NF) membranes are often used in tertiary treatment for water reuse applications given their great salt rejection and efficiency in physically removing pathogens, especially viruses [1]. However, their performance, as inferred from the theoretically predicted values, is far from real operation data because of potential manufacturing/operation induced defects. The mechanical imperfections are undetected during the quality control checks which are part of the manufacturing process.

Hence, the presence or development of membrane element breaches of relatively large size might be detected by monitoring the product water conductivity. However, the development of smaller imperfections not producing measurable changes in conductivity could cause breakthrough of pathogens at undesirable levels. In order to protect public health, these high-pressure membranes must be monitored (ideally online) to ensure their correct operation.

Integrity of the RO membrane can be monitored by direct integrity tests, such as pressure tests, and indirect integrity tests, including turbidity monitoring, on-line conductivity and Total Organic Carbon (TOC) measurements [6]. As per United States Environmental Protection Agency (2005), direct monitoring and indirect monitoring techniques can be employed as real time measurements. The decline in membrane integrity indicates declining membrane functionality in terms of permeability and rejection efficiency. Alteration in the physical properties of the membranes due to creation of scratches and/or holes by crystalline scale material travelling through the spiral-wound interspace for example, and variation in thickness, roughness and chemical structure of the membrane is inevitable during the RO filtration process. Many studies have been conducted to explore the loss of integrity and performance of RO membranes by fouling, scaling and ageing [2-7].

RO membranes provide a barrier for inorganic and organic contaminants including viruses. To date and despite decades of research and operation efforts, there is no ideal approach to accurately detect the actual performance of the filtration systems in terms of virus removal [8,9]. This problem encompasses two aspects: the method itself, coupling an adequate virus surrogate and its suitable detection, and the availability of reproducibly impaired membranes, to serve as comprehensible models for challenge tests.

While manufacturing chemically impaired membranes is more accessible [5-12], although governed by mechanisms not fully understood, the production of mechanically impaired membranes have been attempted for a more reduced number of times and with minimal success rates in terms of defects uniformity or depth of penetration [13-16]. Some of these trials were done using metal needles which produced holes of hundreds of micrometres in diameter, while the needle produced holes tended to tear, showed unstable torn edges and odd shapes. Single laser holes are first investigated by Pontius et al. However, they only mention the proprietary nature of manufacturing details and laser operation; also, their study focused only on ultrafiltration (UF) and microfiltration (MF) membranes.

A study employing intact and pinhole compromised membranes for the removal of MS2 bacteriophages and fluorescent dye polystyrene microspheres estimated that the passage of these surrogates through a pinhole has increased, while rejection efficiency of the compromised membrane declined with increasing hole diameter in cross flow [15]. Some of the experiments have employed compromised UF membranes with 2 pinholes to monitor the virus removal [14,16]. Real-time monitoring of RO membrane integrity by hypodermic needle induced physical disruption revealed higher salt rejection for larger diameter pinhole [17]. To the best of our knowledge our literature review has failed to identify studies of laser impaired RO membranes. This comes to show that there

is a significant knowledge gap in both fundamental and applied research with regards to RO impaired membranes.

The development of more sophisticated laser tools, such as the femtosecond laser ablation systems (Nanoscribe GmbH) [18] lead recently to the fabrication of arrays micro-holes of desired size and number in a relatively large number of materials, such as: polycarbonate, polyethylene, polyethylene-terephthalate, poly-methyl methacrylate and polystyrene. Our preliminary trials employing the same equipment and similar conditions, on commercially available RO membranes, produced large craters in the thin film composite, possibly due to a more energetic interaction between the polyamide/polysulphone and the near infrared (NIR) laser.

In order to avoid the challenges posed by the NIR laser, we employed a MicroPREP Pro-laser ablation system (3D -Micromac), equipped with a nanosecond pulse 532 nm laser which can be used to ablate large domains (centimetres square) while controlling power density and Z motion. The here described method was employed to manufacture arrays of membrane defects (various number of holes and hole depths). Given the similar make of polyamide/polysulphone composite, our method has the potential to be used for the impairment of forward osmosis membranes.

Materials and procedure

The membrane used for the study was a Dow Filmtec BW 30 - 4040 membrane disk of 14.6 cm² (placed over a porous plate). The membranes selected and cut for the study were soaked 24 h in MilliQ water (Millipore Q-POD; conductivity > 18.2 MΩ•cm @ 25 °C) water in a Petri dish and stored at 4 °C. Permeate was collected in beaker placed over an AND GX-4000 electronic weighing balance connected to a computer (RsWeight 5.40 software allowed recording permeate mass every second). Virgin and impaired membranes were used to filter deionised water for two hours at a constant pressure of 12 bars (to compress the membrane). Deionised water filtration (at similar conditions) was followed by sodium chloride solution (2000 ppm; Analytical reagent, Ajax Finechem Pty Ltd) filtration. The membrane coupons needed to be dried before loading into the laser ablation machine. However, the drying of membrane coupons post baseline data acquisition led to a significant drop in performance which was confirmed during testing of the rehydrated coupons (data not shown). Therefore, three membrane coupons were used to determine the baseline performance, and four different membrane coupons cut of the same leaf of the membrane module were used for laser ablation followed by hydration and filtration testing. Salt rejection tests were done for 20 to 30 min with conductivity being measured every 5 min. Laboratory temperature was maintained at 23 °C.

Automatic membrane laser ablation

MicroPREP Pro-laser ablation system (3D-Micromac) equipped with a nanosecond pulse 532 nm laser was employed for membrane impairment. Its proprietary software allowed for creating recipes with control over dimension and number of holes, pulse density and laser power. While this system is typically employed to smooth samples for electron microscopy, we used it to produce four samples (A-D) with 90 holes/20 pulses per μm² (A), 180 holes/2 pulses per μm² (B), 900 holes/0.2 pulses per μm² (C) and 900 holes/0.05 pulses per μm² (D).

Dead-end filtration

The equipment used for filtration testing was a Sterlitech HP4750 Dead End Filtration Unit. Pressurisation was achieved using a compressed Coregas 3.0 type cylinder of >99.9% pure nitrogen. The stirred dead-end filtration cell was a cylindrical stainless-steel column, which can hold up to 300 ml of fluid.

Scanning electron microscopy

All SEM micrographs were acquired employing a variable pressure Hitachi 3500 SEM, operated at moderate accelerating voltage (8 kV) to allow imaging without conductive metal/carbon coating.

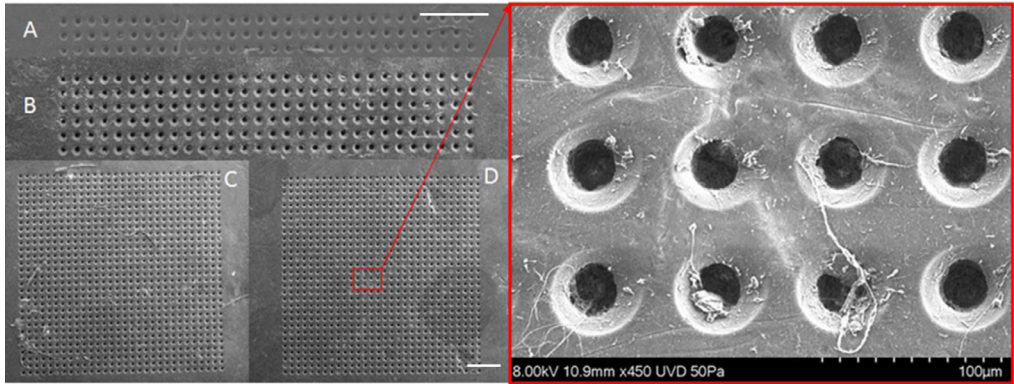


Fig. 1. Top-view SEM micrographs of RO membrane samples (A-D, scalebars of 500 μm) and close-up (right) of holes array in sample D.

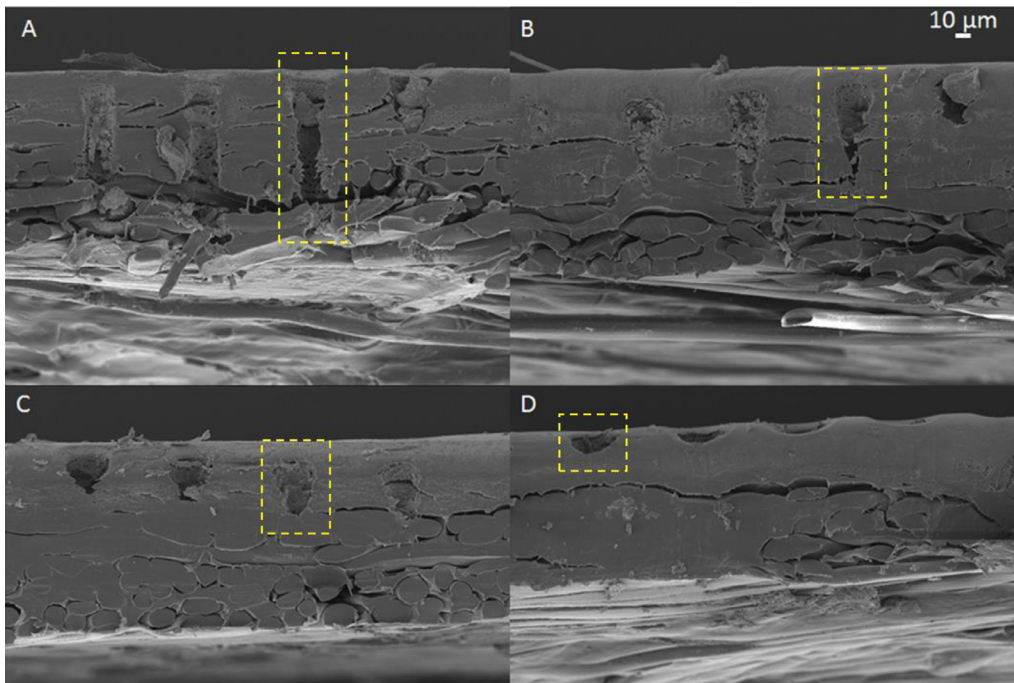


Fig. 2. Cross-section SEM micrographs of surgical blade cut RO membrane samples (A-D; A-20 pulses/ μm^2 , B-2 pulses/ μm^2 , C-0.2 pulses/ μm^2 , D-0.05 pulses/ μm^2). Yellow squares highlight laser penetration through the thin film composite layers.

Method validation

Manufactured arrays of defects

Fig. 1 shows a top-view of the four membranes, revealing uniform size of the produced holes and uniform spacing of 70 μm and hole radius of $13.5 \pm 0.5 \mu\text{m}$. While top-view reveals consistency of the defect manufacturing, surgical blade cross-section of the membranes discloses in **Fig. 2** information

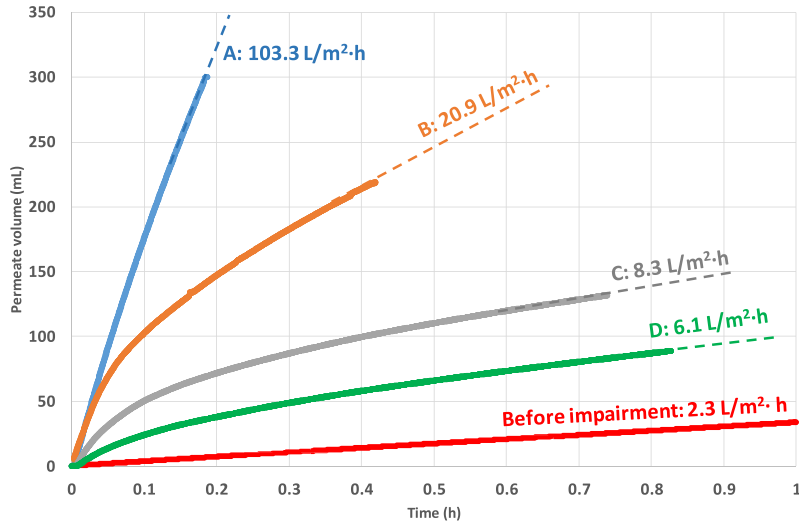


Fig. 3. Membrane performance before and after impairment measured for deionised water (A–D). Terminal flux values were measured on the linear part of the trends.

about laser penetration depth (10–170 μm from sample D to A), directly proportional with the pulse dose, so that, 20 $\text{p}/\mu\text{m}^2$ in the case of sample A is enough to ablate all three layers of the thin film composite membrane, whereas in sample D 0.05 $\text{p}/\mu\text{m}^2$ produces less damage, only on the very top layer of the thin film composite. Although imperfect now, our method could be used with further optimisation to improve selectivity of ablation in terms of hole size and penetration depth.

Impact of impairment on membrane performance

In order to assess the impact of impairment, baseline performance before ablation (water and saline solution flux and salt rejection) was recorded using freshly cut membrane coupons.

Data in Fig. 3 shows an approximately 50 times increase in water permeability between virgin membrane and impaired membrane A (90 holes, all way through penetration). An intermediate permeability of 20.9 $\text{L}/\text{m}^2\cdot\text{h}$ is recorded for membrane B (180 holes, reaching the polysulphone layer). This comes to suggest that the depth of the ablated channel/extent of the damage has a critical impact on performance, surpassing in this stage the number of holes/areas of damage. Even more, samples C, D, having 900 holes each and superficial damage depth, show gradually decreasing permeability.

While before impairment a linear trend is recorded for permeate volume vs time, in the case of impaired membranes A–D, and more pronounced for B, C and D, one can observe a rapid increase of the flux, followed by a saturation/steady zone. Such behaviour could be related to the further compression of the support layer and subsequent hydration/equilibration of polysulphone.

The same membranes used to assess impairment effect on water flux were employed to tests saline solutions flux. Fig. 4 shows a similar factor of 50 for the ratio of virgin membrane saline flux before impairment and sample A (90 deep holes).

In terms of salt rejection (measured by monitoring the conductivity of the permeate), all impaired membranes retained rejections above 99.8% (virgin membrane before impairment: 99.9%; Sample A: 99.8%; Sample B: 99.8%; Sample C and D: 99.9%). In addition to the flux results, these data come to support the hypothesis that although impaired, the polysulphone layer is able to prevent salt passage due to its potential collapse.

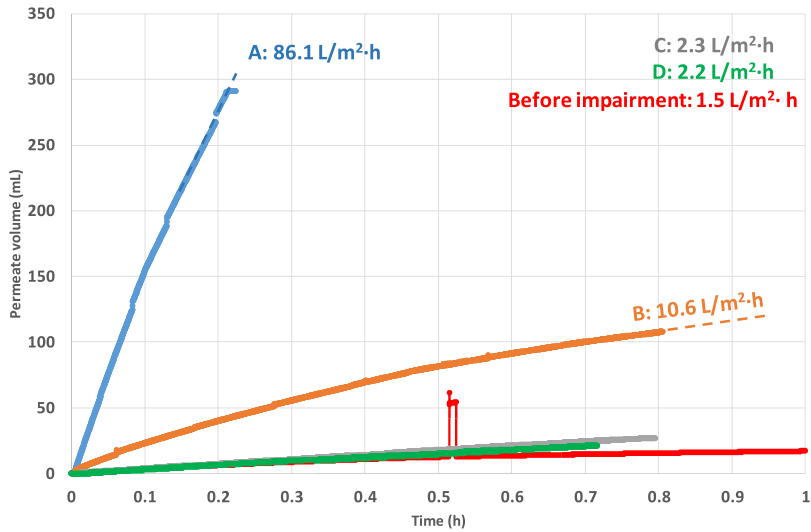


Fig. 4. Membrane performance before and after impairment measured for saline solutions (A–D). Terminal flux values were measured on the linear part of the trends.

Acknowledgments

This work is supported and funded by ARC-Linkage grant [LP160101294](#) and by the [University of Queensland](#) Centre for Natural Gas. This work was performed in part at the Queensland Node of the [Australian National Fabrication Facility](#), a company established under the National Collaborative Research Infrastructure Strategy to provide nano and micro-fabrication facilities for Australia's researchers. The authors acknowledge the facilities and the scientific and technical assistance of the Australian Microscopy & Microanalysis Research Facility at the Centre for Microscopy and Microanalysis (The University of Queensland). BD thanks to Dr Zibin Chen for assistance with laser ablation.

Declaration of Competing Interest

The authors declare that they have no known competing financial interests or personal relationships that could have appeared to influence the work reported in this paper.

Supplementary materials

Supplementary material associated with this article can be found, in the online version, at doi:[10.1016/j.mex.2020.100830](#).

References

- [1] M.A. Shannon, et al., Science and technology for water purification in the coming decades, *Nature* 452 (2008) 301.
- [2] Y. Liu, X. Chen, High permeability and salt rejection reverse osmosis by a zeolite nano-membrane, *Phys. Chem. Chem. Phys.* 15 (18) (2013) 6817–6824.
- [3] H. Hagihara, et al., Depth profiling of the free-volume holes in cellulose triacetate hollow-fiber membranes for reverse osmosis by means of variable-energy positron annihilation lifetime spectroscopy, *Desalination* 344 (2014) 86–89.
- [4] M. Ding, et al., Structure and dynamics of water confined in a polyamide reverse-osmosis membrane: a molecular-simulation study, *J. Memb. Sci.* 458 (2014) 236–244.
- [5] M.-L. Pype, et al., Virus removal and integrity in aged ro membranes, *Water Res.* 90 (2016) 167–175.
- [6] M.-L. Pype, et al., Is ageing hard? a study of aged ro membranes and their integrity to remove virus surrogates, in: 8th International Membrane Science and Technology Conference (IMSTEC 2013), Melbourne, Australia, 2013.

- [7] B.C. Donose, et al., Effect of pH on the ageing of reverse osmosis membranes upon exposure to hypochlorite, *Desalination* 309 (2013) 97–105.
- [8] M.-L. Pype, et al., Reverse osmosis integrity monitoring in water reuse: the challenge to verify virus removal – A review, *Water Res.* 98 (2016) 384–395.
- [9] E.R. Ostarcevic, et al., Current and emerging techniques for high-pressure membrane integrity testing, *Membranes* 8 (3) (2018) 60.
- [10] M.-L. Pype, et al., Fluorescence excitation-emission: a new tool for monitoring the integrity of reverse osmosis membranes? in: IWA-MTC 2011: 6th IWA Specialist Conference on Membrane Technology for Water & Wastewater Treatment, Aachen, Germany, 2011.
- [11] M.-L. Pype, et al., Monitoring reverse osmosis performance: conductivity versus fluorescence excitation–emission matrix (EEM), *J. Memb. Sci.* 428 (2013) 205–211.
- [12] M.-L. Pype, et al., Influence of different reverse osmosis membrane impairments on the rejection behaviour of virus surrogates – lab-scale study, in: 2013 AMTA/AWWA Membrane Technology Conference and Exposition, San Antonio Texas, U.S., 2013, pp. 195–203.
- [13] F.W. Pontius, J.P. Crimaldi, G.L. Amy, Virus passage through compromised low-pressure membranes: a particle tracking model, *J. Memb. Sci.* 379 (1) (2011) 249–259.
- [14] A. Antony, et al., Non-microbial indicators for monitoring virus removal by ultrafiltration membranes, *J. Memb. Sci.* 454 (2014) 193–199.
- [15] B. Mi, et al., Removal of biological and non-biological viral surrogates by spiral-wound reverse osmosis membrane elements with intact and compromised integrity, *Water Res.* 38 (18) (2004) 3821–3832.
- [16] V.S. Frenkel, Y. Cohen, New techniques for real-time monitoring of reverse osmosis membrane integrity for virus removal, *Water Pract. Technol.* 13 (4) (2018) 947–957.
- [17] S. Surawanjitt, Real-Time Monitoring of Reverse Osmosis Membrane Integrity, University of California, 2015.
- [18] C. Liao, et al., Maskless 3D ablation of precise microhole structures in plastics using femtosecond laser pulses, *ACS Appl. Mater. Interfaces* 10 (4) (2018) 4315–4323.